IOSR Journal of Mechanical and Civil Engineering (IOSR-JMCE)
e-ISSN: 2278-1684,p-ISSN: 2320-334X, Volume 13, Issue 1 Ver. I (Jan. - Feb. 2016), PP 79-84
www.iosrjournals.org

Determination of drag coefficient for a passenger car model (Mercedes SEL 300) using the strain gauge method

Abdessamed Kacem, Ali Najim Abdullah
[1] *Ministry Of Higher Education/ Baghdad University*
[2]*Ministry Of Higher Education/ Al-Rafidain University College*

Abstract: *The flow field around an automobile is very complex, characterized by a high degree of three dimensionality, flow separation, reattachment and vortex formation. Flow visualization as well as flow simulation are helpful tools during the aerodynamic design of vehicles.*

The research-undertaken deals with an experimental estimation of C_D (drag coefficient) for Mercedes car, type SEL 300 (scale 1/20) using the strain gauge method (FLA-6-11 type, 120Ω, 2.12 gauge factor, half-bridge connection), which was proved to be practical and reasonably accurate. Experiments were run within a subsonic aspiration wind tunnel, covering an air speed up to 33 m/s (i.e., Reynolds number 6.6 x 10^5). Results for drag coefficient were obtained in the range of 0.37 to 0.19. It was noted that the magnitude of C_D decreased from 0.37 at 21.17 m/s to 0.19 at 33.00 m/s (i.e., decrease of drag coefficient by about 50%). Comparison of our results with those given by other authors is satisfactory.

Key words: *Strain gauge, Drag coefficient, Wind tunnel, Aerodynamics of automobile, Static loading, Dynamic loading, Half bridge connection.*

I. Introduction

Recently the incentive to reduce the aerodynamic drag of road vehicles has increased again. Different methods to estimate drag coefficient of cars have been utilized in the past [1,2]. In the present paper, we use strain gauges with bending moment diagram in order to estimate drag coefficient, the matter that proved to be practical, accurate, and easy.

It is known that loads acting transversely to the plane of a large dimension cause a member to bend. A bar member subjected to this loading is called a beam. In order to resist these loads, a beam must be supported at one or positions along its length. If a beam has one end built-in, it is called a cantilever[3]. We used this idea in order to fix a model of a vehicle at a free end of a cantilever, and estimate the drag coefficient from bending moment diagram of the beam.

II. The Experimental Equipment and Instrumentation

A subsonic wind tunnel, aspiration type, with a maximum speed of 33 m/s, was used. Its cross section and active length are respectively: 230x230 mm^2 and 500mm [4]. Four strain gauges, FLA-6-11, 120 Ω, 2.12 ±1% gauge factor, wire gauge type were used, with adhesive P-2, and coefficient of thermal expansion=$11.8x10^{-6}/^oC$. The temperature coefficient of gauge factor is $+0.1\pm0.05\%/10^oC$ [5]. The sting made of hot rolled, medium carbon steel (0.45%C), damped effect, E= $203.4x10^9$ N/m^2, and $I_z=1.4426x10^{-10}$ m^4.

A model reproducing a Mercedes SEL 300, made from PVC, scale 1/20, and blockage ratio of 16% was tested. The extensometer bridge which was used, was provided with internal impedance of 120Ω to 500Ω, the range of ±20000 points, maximum resolution:1μΩ/Ω, and Amplificatory linearity is 0.002%. The gauge factor regulator is 1 to 5 for 4 digits, and the excitation stability is 0.01%. The branching type is a half-bridge and full-bridge with analogical exit of 0-2V for 0-20000 μΩ/Ω. The minimum charge is 2000Ω, and passer band of analogical exit is 0 to 10 KHz[6].

III. The Experimental Procedure

Dimensions of the sting were chosen so as to reproduce minimum strain that we can read it via strain gauges. The model was fixed at the reference point of the sting as shown schematically in (fig.1a).

From the bending moment diagram, (fig.1b), we can write $M_o=F_Y.X_C + F_X.Y_C$. The value of $(F_Y.X_C)$ approaches to zero[3]. We need two equations in order to find the two unknowns F_X and M_O, and these two equations could be obtained via the sting in its vertical position. Experimental procedure for Mercedes SEL300 model is shown in fig.(2).

1-3-1 Drag force and fluid velocity calculation

The model and four strain gauges were fixed-as shown before in (fig.1a)-at reference point (O), (B), and (A) respectively. L_a is the distance of strain gauge (A) from the reference point (O). L_b is the distance of strain gauge (B) from the reference point (O). From the bending moment diagram, (fig.1b), we have:

$$M_A=M_O + F_X.L_a \quad (1)$$

$$M_B=M_O + F_X.L_b \quad (2)$$

M_A, M_B have direct relationship with readings of strain gauges ε_A, ε_B respectively as shown in subsequent equations:

$$\varepsilon_A = \sigma_A/E = M_A.h/ 2 I_z .E \Longrightarrow M_A = 2I_zE\varepsilon_A/h \quad (3)$$

$$\varepsilon_B = \sigma_B/E = M_B.h/ 2 I_z.E \Longrightarrow M_B =2I_zE\varepsilon_B/h \quad (4)$$

Where I_z represents the second moment of area for the sting around Z-axis as shown schematically in (fig.3). By solving equations (1) and (2), we can find the unknowns F_X and M_O. Drag coefficient could be estimated by the relationship:

$$C_D= F_X/ 0.5\rho V_\infty^2 A \quad (5)$$

And fluid velocity (air-speed) could be estimated by:

$$V_\infty = \sqrt{2g(\rho_w / \rho_a)\Delta h} \quad (6)$$

1-3-2 Deviation analysis for measurements

From equation (6):

$$V= \text{constant x } \sqrt{H}$$

$$\ln V= \ln \text{constant} + \ln H^{1/2} \quad (7)$$

By differentiating the equation logarithmically

$$dV/V = 0.5 \text{ x } dH/H$$

Where dH represents the absolute error ratio in total pressure head that could be estimated:

$$dH = \sqrt{(H - H_m)^2 + (\delta H)^2}$$

Where H represents the total head.

Deviation analysis for drag force measurements could be estimated from:

$$dF_X/ F_X = \pm\sqrt{(d\varepsilon_A / \varepsilon_A)^2 + (d\varepsilon_B / \varepsilon_B)^2} \quad (8)$$

Deviation analysis for drag coefficient could be estimated from:

$$dC_D/C_D = \pm\sqrt{(dF_X / F_X)^2 + (2dV / V)^2} \quad (9)$$

IV. Results and discussion

Experiments were run at an air speed from 21.17 m/s to 33.00 m/s (i.e., Reynolds number from 4.2 10^5 to 6.5 10^5 as shown in figure (6). Results for drag coefficient were obtained in the range of 0.37 to 0.19 as shown in figure (7). It was noted that the value of CD decreased from 0.37 at 21.17 m/s to 0.19 at 33.00 m/s (i.e., decrease of drag coefficient by about 50% within the range of an air speed of 12 m/s).

Such low drag coefficient value of 0.19 is due to the effects by of backlight, which are eliminated on the axial force reduction that resulted from its existence. Figures (4) and (5) show that the flow around the model generates a wake vortex system. There are four distinct vortices in this system. Air coming off the top or rear deck, curves downward to curl back toward the back panel to generate the standing vortex A. Analogously a similar vortex B is formed by air coming upward from underneath the car. Usually the core of the upper vortex A will be downstream from that of B. Similarly, horizontal vortices C are formed at the junction of the sides and back of the body. These are attached to the body and travel with it. These results agree with those of reference [7] (It is believed that all sedan type automobile generate an aerodynamic lift effect which creates the trailing vortices that spiral downstream from the body).

Figure (8) shows that dV/V ratio varies from ± 3.57% to ± 1.47 % (i.e., decreases by 59%), while dF_X/F_X varies from ± 3.55% to ± 1.41 % (i.e., decreases by 60 %), and dC_D/C_D ratio varies from ± 7.79 % to ± 3.26 % (i.e., decreases by 59 %), at the working range of an air speed.

V. Conclusion

The result of this method are extremely encouraging. The method is, therefore, a viable investigation tool that can be used to determine drag coefficient for automobiles. Furthermore, lift coefficient could be estimated at the same way in horizontal position for the sting. Other models, either in aeronautic or building applications could be tested sufficiently, and easily using this method.

Notations

F_X: Total drag force (N).
F_Y: Lift force (N).
M_A: moment at A (N.m).
M_B: moment at B (N.m).
M_O: Pitching moment (N.m).
ε_A: Strain at strain gauge A (μ strain).
ε_B: Strain at strain gauge B (μ strain).
E: Young modulus of elasticity (N/m^2).
(X_C,Y_C):Centroid co-ordinates of the sting.
I_z: Second moment of area (m^4).
σ_A: Stress at A (N/m^2).
σ_B: Stress at B (N/m^2).
b: Width of beam (m).
h: Thickness of beam (m).
ρ_a: Air density (kg/m^3).
ρ_w: Water density (kg/m^3).
V_∞: Undisturbed air flow (m/s).
g: Gravitational acceleration (m/s^2).
Δh: Head difference (m H_2O).
C_D: Drag coefficient.
A: The model frontal area (m^2).
L_a: The distance of strain gauge A from the reference point (O).
L_b: The distance of strain gauge B from the reference point (O).
Subscript (O): Reference point (model fixing position on the sting at the back of the model).

References

[1]. Itsuhei Kohri, Teppei Yamanashi & Takayoshi Nasu, "Study on the transient behavior of the vortex structure behind Ahmed body",SAE 2014.
[2]. Muzafferuddin Mahmood,"flow visualization in Wind Tunnels", 2011.
[3]. M.J.Iremonger,"Basic Stress Analysis", 1984.
[4]. DeltaΔLab, " Soufflerie Subsonique a aspiration EA600", France 2014.
[5]. Tokyo Sokki Kenkyujo Co. "TML Strain Gauge Test Data", Japan,2015.
[6]. DeltaΔLab, " Pont D'Extensometrie EI 616", France 2014.
[7]. Mohan Jagadeesh Kumar M, Anoop Dubey,Shashank Chheniya &Amar jadhav,"Effect of vortex generators on Aerodynamics of a car: CFD Analysis", International Journal of Innovations in Engineering and Technology (IJIET),2013.

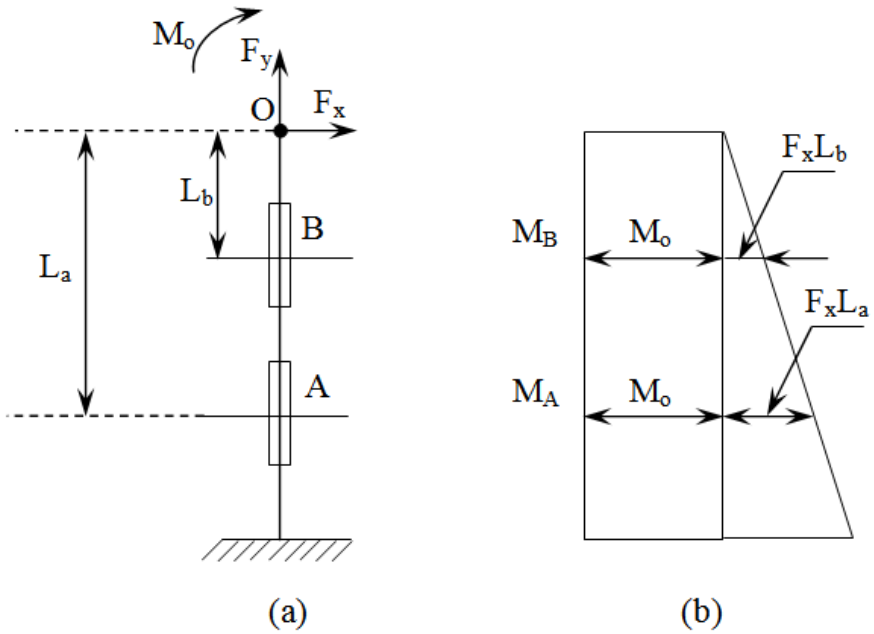

Figure (1): (a) The vertical position of the sting (schematically)
(b) The bending moment diagram for the sting

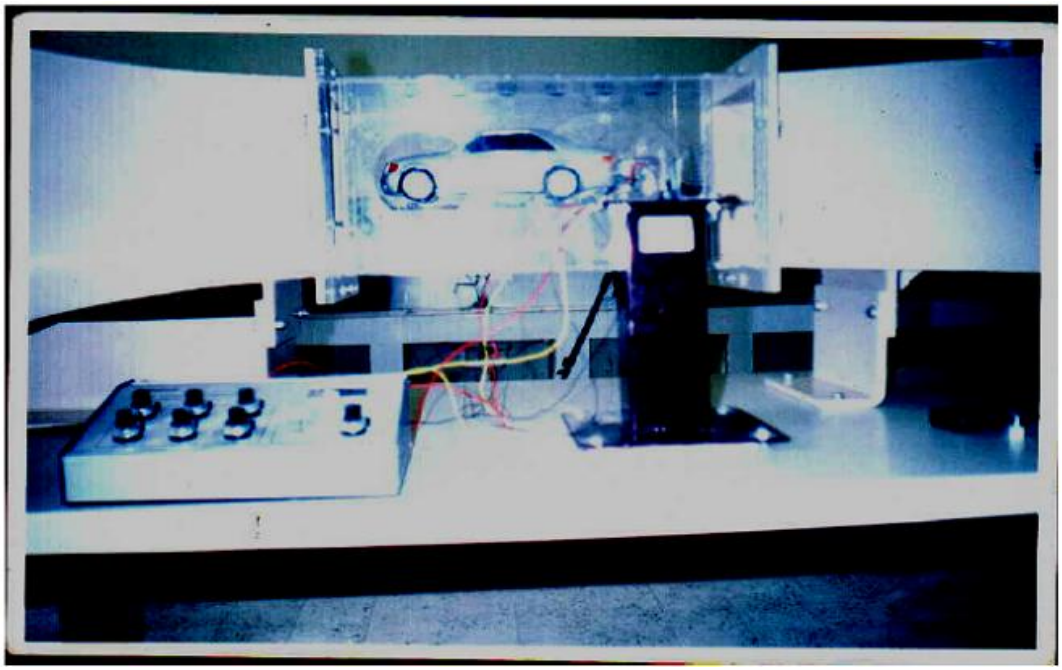

Figure (2): Experimental procedure for Mercedes SEL300 model

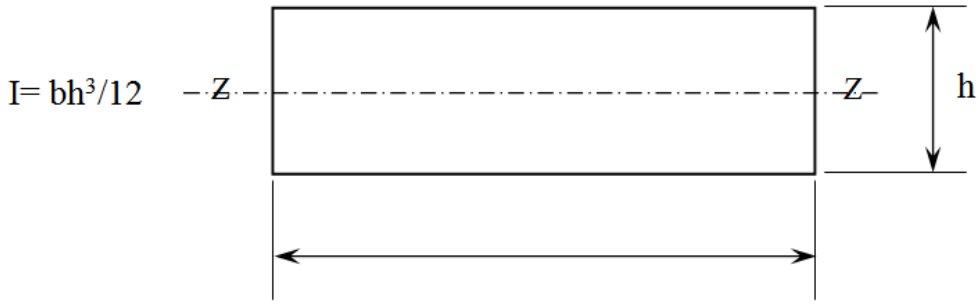

Figure (3): The second moment of area for the sting

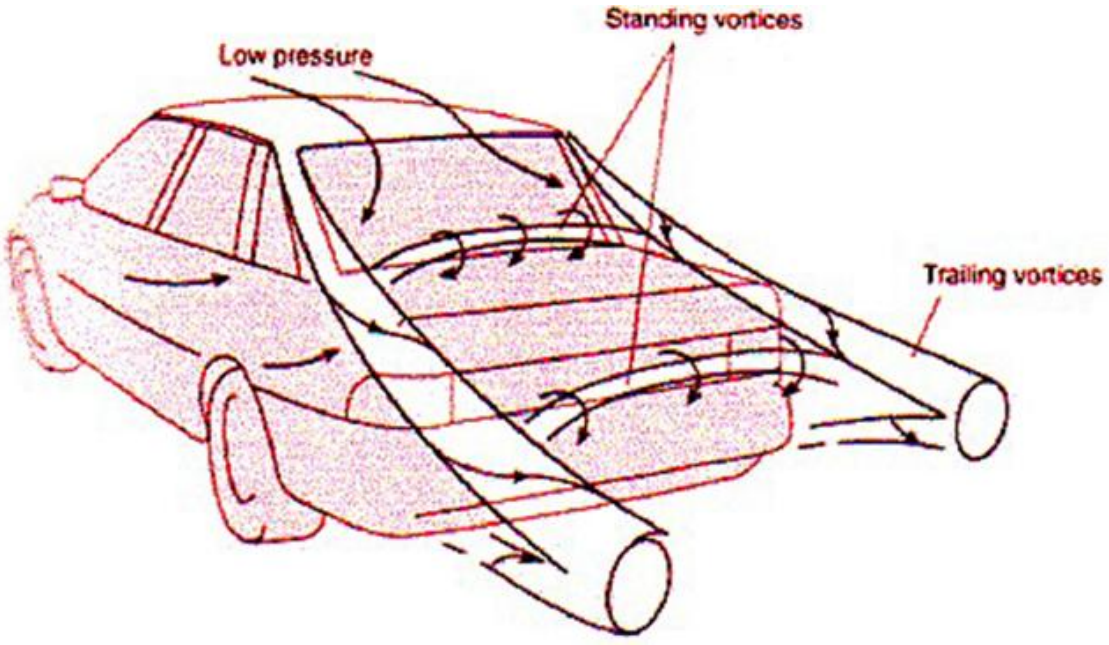

Figure (4): Scheme for the trailing vortices at the rear part of the vehicle

Figure (5) Flow visualization around Mercedes SEL 300 model

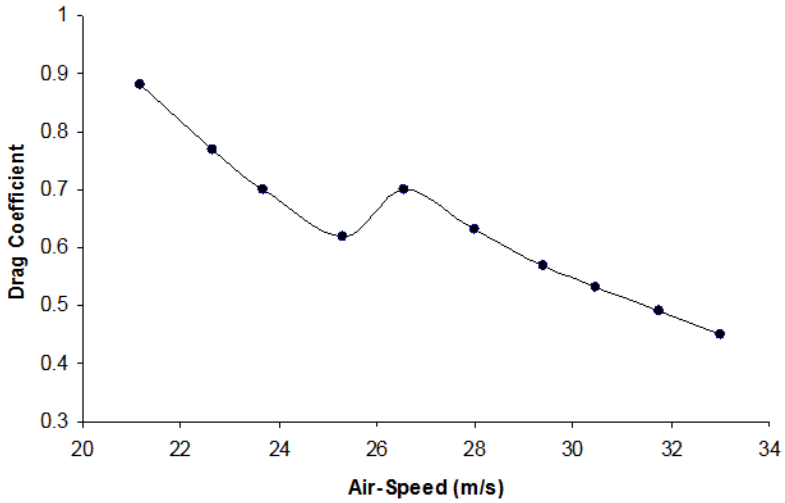

Figure (6): Drag coefficient versus air speed

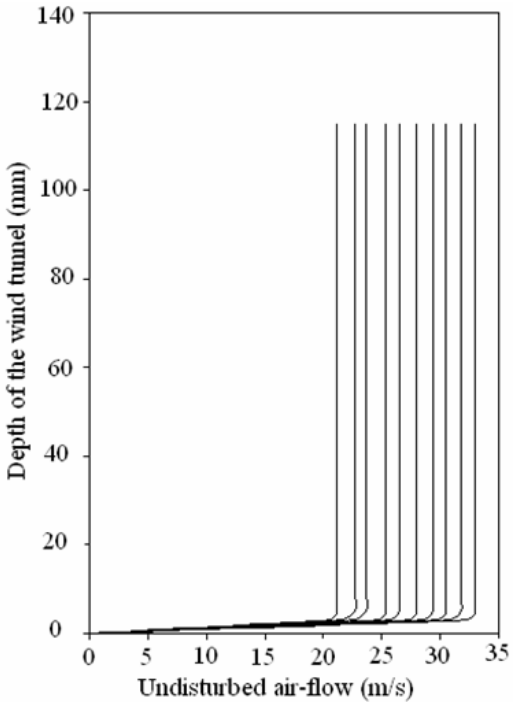

Figure (7) Velocity distribution within the test section.
From calibration of the wind tunnel

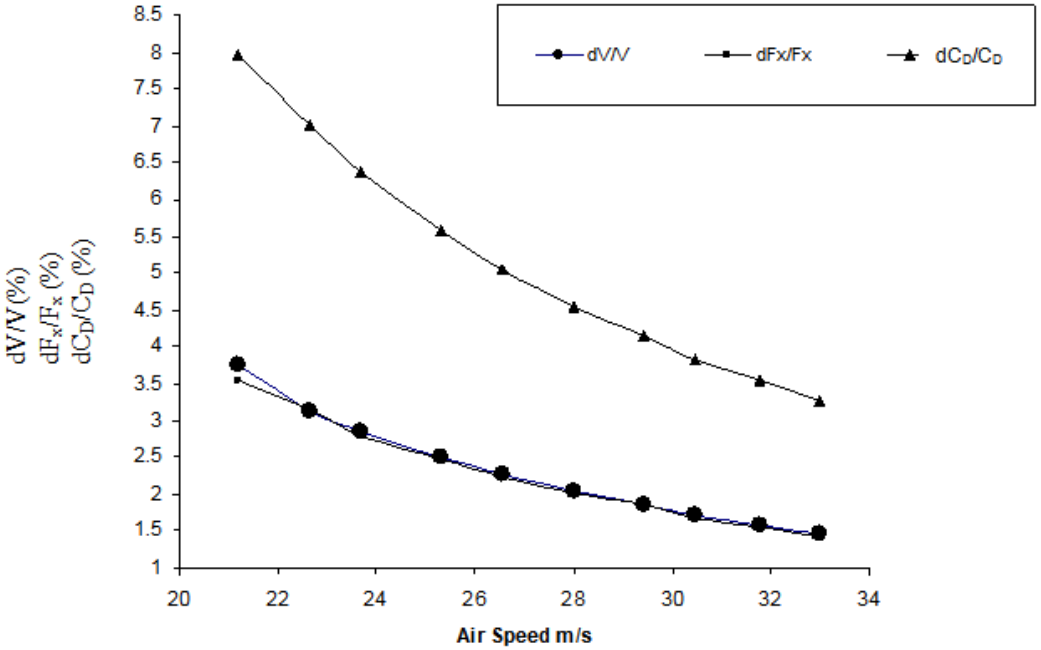

Figure (8): Variation of errors deviation with an air-speed for Mercedes SEL 300 model